TECHNICAL RESEARCH REPORT

SYSTEMS RESEARCH CENTER

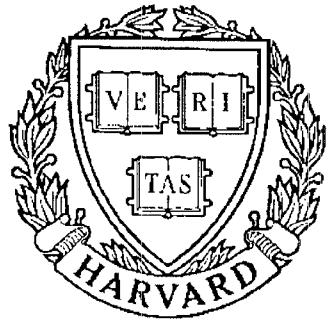

Supported by the National Science Foundation Engineering Research Center Program (NSFD CD 8803012), Industry and the University

On the Redundant-Drive Backlash-Free Robotic Mechanisma

by S.L. Chang and L.W. Tsai

TR 90-38

On the Redundant-Drive Backlash-Free Robotic Mechanisms

Sun-Lai Chang
Graduate Research Assistant

Lung-Wen Tsai
Associate Professor

Mechanical Engineering Department
and
Systems Research Center
The University of Maryland
College Park, MD 20742

Abstract

In this paper, we introduce a new and innovative concept for the control of backlash in gear-coupled robotic mechanisms. The concept utilizes redundant unidirectional drives to assure positive coupling of gear meshes at all times. Based on this concept, a methodology for the enumeration of admissible redundant-drive backlash-free robotic mechanisms has been established. Some typical two- and three-DOF mechanisms have been sketched. Furthermore, actuator torques have been derived as functions of either joint torques or end-effector dynamic performance requirements. A redundantly driven manipulator has the fail-safe advantage in that, except of the loss of backlash control, it can continue to function when one of its actuators fails. It does not have the compliance problem associated with tendon-driven manipulators. A two-DOF backlash-free experimental arm is currently under construction to demonstrate the principle.

1. Introduction

The position and orientation errors of a manipulator are primarily caused by deviations of geometric and non-geometric parameters from their nominal dimensions. Geometric errors arise from machining and assembling of mechanical parts. Non-geometric errors come from joint angle deviations caused by inaccurate encoder readings, mechanical clearances, compliance, backlash, and link deflection due to loading. Various studies on improving positioning accuracy have been published recently by Ahmad (1985), Broderick and Cipra (1988), Chao and Yang (1986), Chen and Chao (1986), Veitschegger and Wu (1986), etc. However, gear backlash control seems to be the topic with least effort because of the difficulty involved with discontinuity and nonlinearity.

Most industrial robots use gear trains for power transmission to allow actuators to be located in some desirable positions. Gear trains are also used for torque amplification. backlash is a persistent problem in such machines due to tooth clearances provided for prevention of jamming of gear teeth due to manufacturing errors or thermal expansion. Backlash introduces discontinuity, uncertainty and impact in mechanical systems which, in turn, makes accurate control of a manipulator difficult. End-effector positioning accuracy is also compromised due to backlash. Precision gears, spring-loaded split gear assemblies, and precise mechanical adjustment are often used to overcome these difficulties. However, these techniques do not completely eliminate the backlash and can increase the cost of manufacturing and assembling. Therefore, further study on reducing or eliminating the backlash problem is urgently needed.

In this paper, we will introduce an innovative concept for the control of gear backlash in robotic mechanisms. Fundamental rules governing the function of redundant-drive backlash-free robotic mechanisms will be presented. Based on these fundamental rules, a number of geared robotic mechanisms

will be enumerated, and actuator torque requirement for this class of robotic mechanisms will be studied.

2. Basic Principle

It is well-known that conventional gears have certain amount of backlash to ensure proper meshing. Backlash can cause momentary loss of coupling between two mating gears whenever there is a torque reversal. This results in positional error and impact in mechanical systems. To overcome the problem, a new technique based on the concept of redundant unidirectional drives is introduced.

Figure 1 shows a one-DOF (degree of freedom) gear train with two unidirectional drives, where D_1 and D_2 are the driving gears and F is the follower. The backlash in this mechanism can be controlled by applying torque to D_1 in a clockwise sense and D_2 in a counter-clockwise sense at all times. The resultant torque acting on F will be in the counter-clockwise or clockwise sense depending on whether torque contributed by D_1 is greater or less than that contributed by D_2. Since no torque reversal is required to drive F, the effects of gear backlash are completely eliminated.

The controllability can be analyzed from kinematic and static points of view. The kinematic equation for the mechanism shown in Fig.1 can be written as:

$$\begin{bmatrix} \phi_1 \\ \phi_2 \end{bmatrix} = \begin{bmatrix} -(N_f/N_1) \\ -(N_f/N_2) \end{bmatrix} \theta, \tag{1}$$

where ϕ_1, ϕ_2 and θ denote the angular displacements of gears D_1, D_2 and F, respectively, and, N_1, N_2 and N_f represent their tooth numbers. Note that the negative sign stands for an external gear mesh. It can be shown that the input and output torques are related by the following equation:

$$\tau_f = \begin{bmatrix} -(N_f/N_1) & -(N_f/N_2) \end{bmatrix} \begin{bmatrix} \xi_1 \\ \xi_2 \end{bmatrix}, \tag{2}$$

where ξ_1 and ξ_2 are the torques applied to D_1 and D_2, respectively, and, τ_f is the output torque of the follower F. For a desired output torque, the applied torques can be expressed as:

$$\begin{bmatrix} \xi_1 \\ \xi_2 \end{bmatrix} = \begin{bmatrix} -\frac{N_1 N_2^2}{N_f(N_1^2+N_2^2)} \\ -\frac{N_1^2 N_2}{N_f(N_1^2+N_2^2)} \end{bmatrix} \tau_f + \lambda \begin{bmatrix} N_1 \\ -N_2 \end{bmatrix}, \tag{3}$$

where λ is an arbitrary real number. The first term on the right-hand-side of Eq. (3) is referred to as the particular solution and the second term the homogenous solution. From Eq. (3), it is clear that by selecting a large positive λ, the sense of input torques $[\ \xi_1 \quad \xi_2\ ]^T$ can be maintained in the $[\ +\ \ -\ ]^T$ direction at all times regardless of the value of τ_f. Similarly, the sense of input torques can also be maintained in the $[\ -\ \ +\ ]^T$ direction by selecting a proper negative λ. We conclude that the mechanism can be controlled by two unidirectional drives which can be designed either in the $[\ +\ \ -\ ]^T$ direction or in the $[\ -\ \ +\ ]^T$ direction.

The principle illustrated in the above simple example can be extended to the case of n-DOF gear-coupled robotic mechanisms with k-unidirectional drives. For an n-DOF articulated mechanism, it can be shown that the input angular displacements and joint angles are related by the following linear transformation:

$$\underline{\phi} = B\ \underline{\theta}, \tag{4}$$

where $\underline{\theta} = [\theta_1, \theta_2, \cdots, \theta_n]^T$ is the joint angular displacement vector,
$\underline{\phi} = [\phi_1, \phi_2, \cdots, \phi_k]^T$ is the input angular displacement vector,
and $B = [b_{ij}]$ is a k by n matrix.

Note that the word *"joint"* refers to the joint in the equivalent open-loop chain of a gear-coupled robotic mechanism. See Tsai (1988) for the definition

of an equivalent open-loop chain. It can also be shown that the equation relating the resultant joint torques to the input torques is given by:

$$\underline{\tau} = B^T \underline{\xi} = A\, \underline{\xi}, \tag{5}$$

where $\underline{\tau} = [\ \tau_1, \tau_2, \cdots, \tau_n\ ]^T$ denotes the resultant joint torques, and $\underline{\xi} = [\ \xi_1, \xi_2, \cdots, \xi_k]^T$ denotes the input actuator torques. The matrix, A, known as the structure matrix, is a function of the structural topology and gear ratios. For a given set of joint torques, Eq. (5) constitutes n linear equations in k unknowns. In order to maintain unidirectional torques in the actuators, k should be greater than n. Thus, the solution for actuator torques consists of a particular solution plus a $(k-n)$ dimensional homogenous solution. The homogenous solution corresponds to certain sets of actuator torques that result in no net joint torques. The homogenous solution can be expressed as a sum of $(k-n)$ basis vectors, each of them being multiplied by an arbitrary constant. Hence, by adjusting the constants, unidirectional actuator torques can be maintained. Furthermore, if $k = n + 1$, then every element in the null vector should be non-zero, and the direction of input torques can be controlled either in the direction of the null vector or in the opposite direction.

3. Enumeration of Redundant-Drive Backlash-Free Robotic Mechanisms

Recently a new methodology, based on the concept of transmission lines, has been developed for the enumeration of gear-coupled robotic mechanisms (Chang and Tsai, 1989). According to the methodology, gear-coupled robotic mechanisms can be created in two steps: (1) enumeration of admissible structure matrices, and (2) construction of mechanisms from the structure matrices. In this paper, we assume that the number of transmission lines is greater than the number of DOF by one, i.e. $k = n + 1$. Hence, the structure matrix

obeys the following fundamental rules:

R1. The structure matrix is an $n \times (n+1)$ matrix and each row must contain at least two non-zero elements.

R2. The sub-matrix obtained by removing any column from a structure matrix is non-singular.

R3. Since actuator torque is transmitted to various joints in a consecutive manner, non-zero elements in a column of the structure matrix must be consecutive.

R4. Switching any two columns of a structure matrix results in a renumbering of the two corresponding input actuators. Hence, two kinematic structures are said to be isomorphic if their corresponding structure matrices become identical after one or repeated operation of column exchanges.

Rules 1 and 2 ensure the unidirectional controllability of a mechanism. Applying the aboves rules, all the admissible structure matrices suitable for redundant-drive backlash-free robotic mechanisms have been enumerated. Table 1 lists four admissible structure matrices for two-DOF mechanisms, where the "#" sign denotes the existence of a non-zero element in the matrix.

Table 2 lists all the admissible 3-DOF structure matrices. In Table 2, the matrices are arranged according to the distribution of actuators. It is assumed that each transmission line has its actuator located on the joint axis nearest to the ground. The letters g, s and e denote that the actuators are to be located on the 1^{st}, 2^{nd} and 3^{rd} joint axes, respectively, and the power stands for the number of actuators to be installed on that joint axis. There are five families listed in Table 2 : g^4, g^3s, g^3e, g^2s^2 and g^2se. For example, the g^4 family allows all the actuators to be ground-connected. The selection of structure matrix is a compromise between mechanical complexity, inertia load, and the coupling, and is not the subject of this study.

The construction of mechanisms from a structure matrix can be accomplished by the method outlined by Chang and Tsai (1989). For example, we can construct a mechanism from structure matrix $g^2s - 2$ listed in Table 1 as follows. First, a transmission line is constructed for each column of the structure matrix as shown in Figs. 2(a), (b) and (c). Then, these transmission lines are combined to form a basic mechanism as depicted in Fig. 2(d). Finally, idler gears can be added to increase the offset distance between two joint axes and/or to achieve greater gear reduction. A derived mechanism is shown in Fig. 3. Note that, many mechanisms can be derived from a basic mechanism. See Chang and Tsai (1989) for the definitions of basic mechanism and derived mechanism.

Figure 4 shows a 3-DOF basic mechanism constructed from the structure matrix of $g^2se - 6$. Figure 5 shows a spatial 3-DOF robot arm derived from the basic mechanism shown in Fig. 4. Figure 6 shows some additional mechanisms constructed from the structure matrices listed in Table 2 where A_i denotes the i^{th} actuator. These mechanisms are judged to be less coupled among each of the five families.

4. Resultant Joint Torques as Functions of Dynamics Performance Criteria

The resultant joint torques as shown in Eq. (5) can be thought of as a set of physical torques acting on the joints of an equivalent open-loop chain. This can be illustrated from the dynamical equations of the system. The Lagrange's equations of motion for a gear-coupled robotic system can be written as:

$$\frac{d}{dt}\left(\frac{\partial L}{\partial \dot{q}_i}\right) - \frac{\partial L}{\partial q_i} = Q_i, \qquad i = 1, 2, \cdots, n \tag{6}$$

$$L = T - V, \tag{7}$$

where the q's denote the generalized coordinates, Q's the generalized active forces and where T and V are the kinetic and potential energies of the system, respectively. Using the joint angles as the generalized coordinates, $q_i = \theta_i$, the generalized active forces can be expressed as:

$$Q_i = \sum_{j=1}^{k} \frac{\partial \phi_j}{\partial q_i} \xi_j, \qquad i = 1, 2, \cdots, n. \tag{8}$$

Taking partial derivatives of Eq. (4) and substituting them into (8), we obtain

$$Q_i = \sum_{j=1}^{k} b_{ji} \xi_j, \qquad i = 1, 2, \cdots, n. \tag{9}$$

Comparing Eqs. (5) and (9), we conclude that the resultant joint torques are the generalized active forces, i.e.

$$Q_i = \tau_i, \qquad i = 1, 2, \cdots, n. \tag{10}$$

The same dynamical equations would be obtained if we assume the mechanism is made up of an open-loop chain having τ_i acting on joint i. Hence, the dynamic response of the system can be completely characterized by the resultant joint torques.

For a given set of joint torques, actuator torques can be obtained by solving Eq. (5):

$$\underline{\xi} = A^{+} \underline{\tau} + \lambda \, \underline{\mu} \tag{11}$$

where $\underline{\mu} = [\mu_1, \mu_2, \cdots, \mu_n]^T$ is the null vector of A, i.e. $A \, \underline{\mu} = \underline{0}$,
$A^{+} = A^T (A \, A^T)^{-1}$ is the pseudo inverse of A,

and where λ is an arbitrary real number (Klein and Huang, 1983). The first term on the right-hand-side of Eq. (11) is called the particular solution

and the second term, which results in no net joint torques, is called the homogenous solution. The orthogonality property between these two terms can be shown as follows:

$$(A^{+}\underline{\tau})^{T}\ \lambda\ \underline{\mu} = \lambda\ \underline{\tau}^{T}\{(A\ A^{T})^{-1}\}^{T}\ A\ \underline{\mu} = 0 \tag{12}$$

Equation (12) implies that the particular solution is a hyperplane passing through the origin and perpendicular to the null vector. To control backlash, actuator torques should be kept in a predetermined direction at all times. This can be achieved by adjusting the arbitrary constant λ. Equation (11) implies that the direction of actuator torques can be kept either in the direction of the null vector or in the opposite direction.

In the design of a manipulator, sometimes it is desirable to specify the performance in terms of its velocities and accelerations at the end-effector. For this purpose, the joint velocities and joint accelerations in Eq. (6) can be replaced by the end-effector velocities and accelerations. Using the inverse kinematic transformation, the resulting equation can be written in the following form (Thomas and Tesar, 1982):

$$\tau_i = G_i^T\ \underline{\alpha} + \underline{v}^T P_i \underline{v} + f_i, \qquad i = 1, 2, \cdots, n, \tag{13}$$

where $\underline{v}$ and $\underline{\alpha}$ are velocity and acceleration vectors of the end-effector, G_i and P_i are $n \times 1$ and $n \times n$ coefficient matrices relating the motion state to joint torques, and f_i is the contribution due to conservative forces. Note that $\underline{v}$ and $\underline{\alpha}$ contain both linear and angular components, and G_i and P_i are position dependent.

Hence, joint torques can be calculated from a set of velocity and acceleration specifications. Since the maximum achievable velocity and acceleration are position dependent, the performance of a manipulator can only be specified at certain position(s) of the end-effector. Since, at a given position, the

maximum velocity and acceleration are also direction dependent, we may specify the performance of a manipulator in terms of its ability to reach

$$\begin{aligned} \underline{v}^T W_v \underline{v} &= v_s^2, \\ \text{and} \quad \underline{\alpha}^T W_\alpha \underline{\alpha} &= a_s^2, \end{aligned} \tag{14}$$

for all directions of motion, where v_s and a_s are the desired magnitudes for the velocity and acceleration, and where W_α and W_v are $n \times n$ symmetric matrices used as weighting functions. If W_α and W_v are chosen to be identity matrices, then Eq. (14) implies that the end-effector can achieve a maximum velocity and acceleration of v_s and a_s, respectively at the specified location. Thomas, et al. (1985) studied the minimum joint torque requirement for optimal actuator sizing based on local dynamic criteria. The study of Thomas, et al. can be applied to individual joint-drive manipulators. However, for gear-coupled mechanisms with unidirectional drives, the theory for actuator sizing is still unexplored. In what follows, the actuator sizing requirement will be studied.

5. Actuator Sizing in Terms of Joint Torques Requirement

Let D_j be the joint torque working domain, in which a manipulator is intended to operate. This working domain must be transformed into the actuator torque domain, D_ξ, in order to size the actuators properly. The transformation from joint torques to input torques can be accomplished in two steps, namely a transformation from the joint torque domain, D_j, to a particular solution hyperplane, D_p, followed by a transformation from the particular solution domain to the actuator torque domain, D_ξ. Figures 7(a) and (b) show the transformation between D_j, D_p, and D_ξ in grapherical form. Note that the transformation from D_j to D_p is unique and D_ξ is obtained by extending D_p along the null vector to plus and minus infinity. For a given set of joint torques $\underline{\tau}^*$ in D_j, there is a particular solution $\underline{\xi}_p^*$ in D_p, and the required motor torques can be any point on the line passing through $\underline{\xi}_p^*$

and parallel to the null vector. To eliminate backlash effects, motor torques must lie in a predetermined quadrant. The actuator sizes can be determined by selecting a proper multiplier, λ, such that corresponding to every point in the joint torque domain, D_p, the required motor torque falls within the predetermined quadrant. Unfortunately, both domains of the working joint torques, D_j, and the particular solution hyperplane, D_p, cannot be descirbed in concise mathematical forms. This method is, therefore, judged to be impractical for actuator sizing. In what follows, we describe an alternate approach.

We propose to size the actuators in a reverse manner. This can be illustrated by taking the 2-DOF mechanism shown in Fig. 3 as an example. The structure matrix of the mechanism shown in Fig. 3 is given by:

$$A = \begin{bmatrix} \frac{N_{17}N_{19}}{N_{18}N_{20}} & \frac{N_{13}N_{15}}{N_{14}N_{16}} & 0 \\ \frac{N_{17}N_{19}N_4N_6}{N_{18}N_{20}N_3N_5} & 0 & -\frac{N_7N_9N_{11}}{N_8N_{10}N_{12}} \end{bmatrix}. \tag{15}$$

Substituting $N_3 = 64$, $N_4 = N_{14} = N_{16} = N_{18} = N_{20} = 16$, $N_5 = N_{12} = 24$, $N_6 = 12$, $N_7 = N_{10} = 20$, $N_8 = 10$, $N_9 = 48$, $N_{11} = 120$, and, $N_{13} = N_{15} = N_{17} = N_{19} = 96$ into Eq. (15), yields

$$A = \begin{bmatrix} 40.96 & 40.96 & 0 \\ 5.12 & 0 & -24 \end{bmatrix}. \tag{16}$$

The null vector of this structure matrix is $[75, -75, 16]^T$. To simplify the analysis, we redefine the positive direction of the 2^{nd} motor axis so that the structure matrix becomes

$$A = \begin{bmatrix} 40.96 & -40.96 & 0 \\ 5.12 & 0 & -24 \end{bmatrix}, \tag{17}$$

and the null vector becomes $[75, 75, 16]^T$. Assuming that the actuators chosen for the mechanism have available torque range of $[\ \pm\hat{\xi}_1,\ \pm\hat{\xi}_2,\ \pm\hat{\xi}_3]^T$, then the domain of actuator torques, $\hat{D}_\xi$, will be a rectangular solid in the first

quadrant as shown in Fig. 8. Projecting $\hat{D}_\xi$ along the direction of the null vector results in a domain, $\hat{D}_p$, in the particular solution hyperplane. The corresponding available joint torque domain, $\hat{D}_j$, can then be obtained by a transformation using Eq. (5). The domain of available joint torques, $\hat{D}_j$ should contain the domain of desired joint torques, D_j, as a subset. To obtain $\hat{D}_p$, all 12 edges of the rectangular solid are projected onto the particular solution hyperplane along the direction of the null vector. But, six of them fall inside the boundary of the others. Hence, only six edges constitute the boundary of $\hat{D}_p$ as shown in Fig. 8. Each of them can be expressed as the intersection of two planes as shown below:

$$\begin{cases} \xi_i = \hat{\xi}_i, & i = 1,2,3 \\ \xi_j = 0, & j = 1,2,3, \quad j \neq i. \end{cases} \tag{18}$$

Substituting Eqs. (17) and (18) into (5) for each combination of (i,j), we obtain two equations linear in ξ_k, $k \neq i \neq j$. We then eliminate ξ_k from the two equations. This results in one equation which serves as one of the boundary lines for the $\hat{D}_j$ domain. Repeating the above process for all combinations of (i,j), we obtain the boundary of the available joint torque domain, $\hat{D}_j$, as shown below:

$$\begin{cases} \tau_1 \geq -40.96\ \hat{\xi}_2 \\ \tau_1 \leq 40.96\ \hat{\xi}_1 \\ \tau_2 \geq -24\ \hat{\xi}_3 \\ \tau_2 \leq 5.12\ \hat{\xi}_1 \\ \tau_1 - 8\ \tau_2 \leq 192\ \hat{\xi}_3 \\ \tau_1 - 8\ \tau_2 \geq -40.96\ \hat{\xi}_2 \end{cases} \tag{19}$$

This domain is sketched in Fig. 9 for the purpose of illustration. Note that we have used a hat, $\hat{}$, to denote the available torques from a set of actuators.

The above methodology can be extended to a general n-DOF robot arm. For the reason of simplicity, we assign the directions of actuator axes in such a way that all elements in the null vector are positive. Thus, the domain of

available motor torques, $\hat{D}_\xi$, can be represented by an $(n+1)$-dimentional rectangular solid in the first quadrant. There are $2n(n+1)$ edges in an $(n+1)$-dimentional rectangular solid. After transformation, only $n(n+1)$ edges form the boundary of $\hat{D}_p$, and each of them can be represented as the intersection of two planes:

$$\begin{cases} \xi_i = 0, & i = 1, 2, \cdots, n+1 \\ \xi_j = \hat{\xi}_j, & j = 1, 2, \cdots, n+1, \quad j \neq i, \end{cases} \tag{20}$$

where $\hat{\xi}_j$ is the maximum available torque from the j^{th} actuator. Substituting Eq. (20) into (5) for each combination of (i, j), we obtain:

$$\underline{\tau} = A_{ij}\underline{\xi}_{ij} + \hat{\xi}_j \; A_j, \tag{21}$$

where A_{ij} is the matrix obtained by deleting the i^{th} and j^{th} columns from matrix A, $\underline{\xi}_{ij}$ is the column matrix obtained by deleting the i^{th} and j^{th} elements from $\underline{\xi}$, and A_j denotes the j^{th} column of matrix A.

Equation (21) represents n linear equations in $(n-1)$ unknowns, $\underline{\xi}_{ij}$, and the compatibility condition for non-trivial solutions to exist is:

$$\left|\underline{\tau} - \hat{\xi}_j A_j \quad A_{ij}\right| = \sum_{l=1}^{n} (-1)^{l-1} (\tau_l - \hat{\xi}_j a_{lj}) \left|A_{ij}^l\right| = 0, \tag{22}$$

where $|(\;)|$ denotes the determinant of $(\;)$, a_{lj} denotes the (l, j) element of A, and A_{ij}^l denotes a sub-matrix of A_{ij} with the l^{th} row omitted. Rearranging Eq. (22) yields the following boundary hyperplanes:

$$\sum_{l=1}^{n} (-1)^{l-1} \tau_l \left|A_{ij}^l\right| = \hat{\xi}_j \sum_{l=1}^{n} (-1)^{l-1} a_{lj} \left|A_{ij}^l\right| = \hat{\xi}_j (-1)^s \left|\hat{A}_i\right|, \tag{23}$$

where $\hat{A}_i$ denotes a sub-matrix of A with the i^{th} column omitted, and where

$$\begin{cases} s = j - 1, & if \;\; i > j \\ s = j, & if \;\; i < j. \end{cases} \tag{24}$$

Hence, the actuator torque requirements can be written as:

$$\hat{\xi}_j \geq (-1)^s \frac{\sum_{l=1}^{n} (-1)^{l-1} \tau_l \left| A_{ij}^l \right|}{\left| \hat{A}_i \right|}, \tag{25}$$

where $i = 1, 2, \cdots, n+1$; $j = 1, 2, \cdots, n+1$; and $j \neq i$. There are $n(n+1)$ such equations. Hence, corresponding to a set of joint torques, Eq. (25) yields the minimum torque requirement for each actuator.

6. Actuator Sizing in Terms of End-Effector Performance Criteria

The actuator torque requirements can be written as functions of end-effector performance criteria. Substituting Eq. (13) into (25), yields:

$$\hat{\xi}_j \geq (-1)^s \frac{\sum_{l=1}^{n} (-1)^{l-1} \left| A_{ij}^l \right| (G_l^T \underline{\alpha} + \underline{v}^T P_l \underline{v} + f_l)}{\left| \hat{A}_i \right|}, \tag{26}$$

or

$$\hat{\xi}_j \geq F_j^T \underline{\alpha}^T + \underline{v}^T H_j \underline{v} + g_j, \qquad j = 1, 2, \cdots, n \tag{27}$$

where

$$F_j^T = (-1)^s \frac{\sum_{l=1}^{n} (-1)^{l-1} \left| A_{ij}^l \right| \; G_l^T}{\left| \hat{A}_i \right|} \tag{28}$$

$$H_j = (-1)^s \frac{\sum_{l=1}^{n} (-1)^{l-1} \left| A_{ij}^l \right| \; P_l}{\left| \hat{A}_i \right|} \tag{29}$$

$$g_j = (-1)^s \frac{\sum_{l=1}^{n} (-1)^{l-1} \left| A_{ij}^l \right| \; f_l}{\left| \hat{A}_i \right|} \tag{30}$$

and $i = 1, 2, \cdots, n+1, \qquad i \neq j.$

The actuators should be selected to satisfy Eq. (14), i.e.

$$\underline{v}^T W_v \underline{v} = v_s^2$$

and $$\underline{\alpha}^T W_\alpha \underline{\alpha} = a_s^2$$

Since the maximum value of the three terms in the right-hand-side of Eq. (27) can occur simultaneously, actuators should be chosen such that their available torques, $\hat{\underline{\xi}}$, are equal to the sum of the maximum value of each term. The maximum value of each term can be obtained as follows:

(a) 1^{st} term:

$$Max \quad \xi_j^\alpha = F_j^T \underline{\alpha}, \quad subject\ to \quad \underline{\alpha}^T W_\alpha \underline{\alpha} = a_s^2 \tag{31}$$

where ξ_j^α denotes the maximum torque required to produce a desired acceleration, $\underline{\alpha}$. Define J as

$$J = F_j^T \underline{\alpha} + h\ (\underline{\alpha}^T W_\alpha \underline{\alpha} - a_s^2), \tag{32}$$

where h is a Lagrange multiplier. Equating $\frac{\partial J}{\partial \underline{\alpha}}$ and $\frac{\partial J}{\partial h}$ to zero, yields:

$$F_j + 2\ h\ W_\alpha \underline{\alpha} = \underline{0}, \tag{33}$$

and

$$\underline{\alpha}^T W_\alpha \underline{\alpha} = a_s^2, \tag{34}$$

Premutiplying Eq. (33) by $\underline{\alpha}^T$ and substitutting (34) into the resulting equation, we obtain

$$F_j^T \underline{\alpha} + 2\ h\ a_s^2 = 0. \tag{35}$$

Thus, the maximum value of ξ_j^α occurs at

$$h = -\frac{F_j^T \alpha}{2a_s^2} = -\frac{\xi_j^\alpha}{2a_s^2}. \tag{36}$$

Substituting Eq. (36) into (33) and simplifying, yields:

$$\underline{\alpha} = \frac{a_s^2 W_\alpha^{-1} F_j}{\xi_j^\alpha} \tag{37}$$

Premultiplying Eq. (37) by F_j^T and simplifying, we obtain the maximum value of ξ_j^α,

$$\xi_j^\alpha = a_s (F_j^T W_\alpha^{-1} F_j)^{\frac{1}{2}}. \tag{38}$$

(b) 2^{nd} term:

$$Max \qquad \xi_j^v = \underline{v}^T H_j \underline{v}, \qquad subject\ to \qquad \underline{v}^T W_v \underline{v} = v_s^2. \tag{39}$$

Define J as

$$J = \underline{v}^T H_j \underline{v} + h\ (\underline{v}^T W_v \underline{v} - v_s^2), \tag{40}$$

where h is a Lagrange mutiplier. By the same method, equating $\frac{\partial J}{\partial \underline{v}}$ and $\frac{\partial J}{\partial h}$ to zero, yields:

$$(H_j + H_j^T)\ \underline{v} + 2\ h\ W_v \underline{v} = \underline{0}, \tag{41}$$

and

$$\underline{v}^T W_v \underline{v} = v_s^2. \tag{42}$$

From Eq. (41), it can be shown that $h = -\frac{1}{2}$ eigenvalue of $W_v^{-1}(H_j + H_j^T)$, and $\underline{v}$ = eigenvector of $W_v^{-1}(H_j + H_j^T)$. Premultiplying Eq. (41) by $\underline{v}^T$ and substituting (42) into the resulting equation, yields

$$\underline{v}^T(H_j + H_j^T)\ \underline{v} + 2\ h\ v_s^2 = 0. \tag{43}$$

Thus, ξ_j^v has a maximum value of

$$\xi_j^v = \underline{v}^T H_j \underline{v} = -\ h\ v_s^2. \tag{44}$$

(c) 3^{rd} term:

The third term is position dependent and can be obtained directly from Eq. (30). Finally, the actuactor sizes can be determined by summing Eqs. (38), (44) and (30).

7. Summary

We have introduced a new and innovative concept for the control of backlash in gear-coupled robotic systems. The concept utilizes redundant unidirectional drives to assure positive coupling of gear meshes at all times.

Based on the concept, we have established a systematic methodology for the enumeration of a class of unidirectional-drive gear-coupled robotic mechanisms. Some typical two- and three-DOF robot manipulators have been sketched for the purpose of demonstration. Actuator sizes have been derived as functions of either joint torques or end-effector dynamic performance requirements.

The main purpose of this concept is the elimination of gear backlash in a manipulator. One of the necessary conditions for the controllability of such a mechanism is that a sub-matrix obtained by deleting any column from the structure matrix is non-singular. Physically, this means that a redundantly driven manipulator has the fail-safe advantage in that, except for the loss of backlash control, it can continue to function when one of its actuators fails to work. Furthermore, if high accuracy is not important between precision points, then it is possible to control the actuators in such a way that no

antagonism exist among the actuators so as to achieve optimal dynamic performance.

Elimination of gear backlash reduces noise and vibration associated with gear trains and, at the same time, improves the accuracy and stability of a manipulator. Since gear trains are structurally much more rigid than cables and tendons, the compliance problem associated with tendon-driven manipulators is also eliminated. The result is a high precision and high performance manipulator.

In order to demonstrate the principle, we have designed a planar two-DOF backlash-free arm as shown in Fig. 3. A controller based on computed position and computed torque tenique is currently being designed. This shall be the subject of a future article.

Acknowledgement

This work was supported in part by the U.S. Department of Energy under Grant DEFG05-88ER13977 and in part by the NSF Engineering Research Centers Program, NSFD CDR 8803012. Such support does not constitute an endorsement by the supporting agencies of the views expressed in the paper.

References:

Ahmad, S., 1985,*"Second Order Nonlinear Kinematic Effects and Their Compensation"*, Proc. of the 1985 IEEE Inter. Conf. on Robotics and Automation, St. Louis, Vol. 2, pp. 307-314.

Broderick, P.L. and Cipra, R.J., 1988, *"A Method for Determining and Correcting Robot Position and Orientation Errors Due to Manufacturing"*, ASME J. of Mechanisms, Transmissions, and Automation in Design, Vol. 110, No. 1, pp. 3-10.

Chang, S.L. and Tsai, L.W., 1989, *"Synthesis and Analysis of Geared Robotic Mechanisms"*, Proc. of the 1989 IEEE Inter. Conf. on Robotics and Automation, Scottsdale, AZ, Vol. 2, pp. 920-927.

Chao, L.M. and Yang, J.C.S., 1986, *"Development and Implementation of a Kinematic Parameter Identification Technique to Improve the Positioning Accuracy of Robots"*, Proceedings of SME Conf. Robots 10, Chicago, Ill.

Chen, J. and Chao, L.M., 1986, *"Positioning Error Analysis for Robot Manipulators with All Rotary Joints"*, Proc. of the 1987 IEEE Inter. Conf. on Robotics and Automation, San Francisco, CA, Vol. 2, pp. 1011-1016.

Klein, C.A. and Huang, C.H., 1983, *"Review of Pseudo-Inverse Control for Use with Kinematically Redundant Manipulators"*, IEEE Trans. on System, Man, and Cybernetics, Vol, SM513, pp. 245-250.

Thomas, M. and Tesar, D., 1982, *"Dynamic Modeling of Serial Manipulator Arms"*, ASME J. of Mechanisms, Transmissions, and Automation in Design, Vol. 104, pp. 218-228.

Thomas, M., Yuan-Chou, H.C. and Tesar, D., 1985, *" Optimal Actuator Sizing for Robotic Manipulators Based on Local Dynamic Criteria"*, ASME J. of Mechanisms, Transmissions, and Automation in Design, Vol. 107, pp. 163-169.

Tsai, L.W., 1988, *"The Kinematics of Spatial Robotic Bevel-Gear Train"*, IEEE J. of Robotics and Automation, Vol. 4, No.2, pp. 150-156.

Veitschegger, W.K. and Wu, C.H., 1986, *"Robot Accuracy Analysis Based on Kinematics"*, IEEE J. of Robotics and Automation, Vol. 2, No. 3, pp. 171-179.

$$\underset{g^3-1}{\begin{bmatrix} \# & \# & \# \\ \# & \# & \# \end{bmatrix}} \qquad \underset{g^3-2}{\begin{bmatrix} \# & \# & \# \\ \# & \# & 0 \end{bmatrix}} \qquad \underset{g^2s-1}{\begin{bmatrix} \# & \# & 0 \\ \# & \# & \# \end{bmatrix}} \qquad \underset{g^2s-2}{\begin{bmatrix} \# & \# & 0 \\ \# & 0 & \# \end{bmatrix}}$$

Table 1 Admissible 2-DOF structure matrices

$$\begin{bmatrix} \# & \# & \# & \# \\ \# & \# & \# & \# \\ \# & \# & \# & \# \end{bmatrix}$$
g^4-1

$$\begin{bmatrix} \# & \# & \# & \# \\ \# & \# & \# & \# \\ \# & \# & \# & 0 \end{bmatrix}$$
g^4-2

$$\begin{bmatrix} \# & \# & \# & \# \\ \# & \# & \# & 0 \\ \# & \# & \# & 0 \end{bmatrix}$$
g^4-3

$$\begin{bmatrix} \# & \# & \# & \# \\ \# & \# & \# & \# \\ \# & \# & 0 & 0 \end{bmatrix}$$
g^4-4

$$\begin{bmatrix} \# & \# & \# & \# \\ \# & \# & \# & 0 \\ \# & \# & 0 & 0 \end{bmatrix}$$
g^4-5

$$\begin{bmatrix} \# & \# & \# & 0 \\ \# & \# & \# & \# \\ \# & \# & \# & \# \end{bmatrix}$$
g^3s-1

$$\begin{bmatrix} \# & \# & \# & 0 \\ \# & \# & \# & \# \\ \# & \# & \# & 0 \end{bmatrix}$$
g^3s-2

$$\begin{bmatrix} \# & \# & \# & 0 \\ \# & \# & \# & \# \\ \# & \# & 0 & \# \end{bmatrix}$$
g^3s-3

$$\begin{bmatrix} \# & \# & \# & 0 \\ \# & \# & \# & \# \\ \# & \# & 0 & 0 \end{bmatrix}$$
g^3s-4

$$\begin{bmatrix} \# & \# & \# & 0 \\ \# & \# & \# & \# \\ \# & 0 & 0 & \# \end{bmatrix}$$
g^3s-5

$$\begin{bmatrix} \# & \# & \# & 0 \\ \# & \# & 0 & \# \\ \# & \# & 0 & \# \end{bmatrix}$$
g^3s-6

$$\begin{bmatrix} \# & \# & \# & 0 \\ \# & \# & 0 & \# \\ \# & \# & 0 & 0 \end{bmatrix}$$
g^3s-7

$$\begin{bmatrix} \# & \# & \# & 0 \\ \# & \# & 0 & \# \\ \# & 0 & 0 & \# \end{bmatrix}$$
g^3s-8

$$\begin{bmatrix} \# & \# & \# & 0 \\ \# & \# & \# & 0 \\ \# & \# & \# & \# \end{bmatrix}$$
g^3e-1

$$\begin{bmatrix} \# & \# & \# & 0 \\ \# & \# & \# & 0 \\ \# & \# & 0 & \# \end{bmatrix}$$
g^3e-2

$$\begin{bmatrix} \# & \# & \# & 0 \\ \# & \# & 0 & 0 \\ \# & \# & 0 & \# \end{bmatrix}$$
g^3e-3

$$\begin{bmatrix} \# & \# & \# & 0 \\ \# & \# & \# & 0 \\ \# & 0 & 0 & \# \end{bmatrix}$$
g^3e-4

$$\begin{bmatrix} \# & \# & \# & 0 \\ \# & \# & 0 & 0 \\ \# & 0 & 0 & \# \end{bmatrix}$$
g^3e-5

$$\begin{bmatrix} \# & \# & 0 & 0 \\ \# & \# & \# & \# \\ \# & \# & \# & \# \end{bmatrix}$$
g^2s^2-1

$$\begin{bmatrix} \# & \# & 0 & 0 \\ \# & \# & \# & \# \\ \# & \# & \# & 0 \end{bmatrix}$$
g^2s^2-2

$$\begin{bmatrix} \# & \# & 0 & 0 \\ \# & \# & \# & \# \\ \# & 0 & \# & \# \end{bmatrix}$$
g^2s^2-3

$$\begin{bmatrix} \# & \# & 0 & 0 \\ \# & \# & \# & \# \\ \# & 0 & \# & 0 \end{bmatrix}$$
g^2s^2-4

$$\begin{bmatrix} \# & \# & 0 & 0 \\ \# & \# & \# & \# \\ 0 & 0 & \# & \# \end{bmatrix}$$
g^2s^2-5

$$\begin{bmatrix} \# & \# & 0 & 0 \\ \# & 0 & \# & \# \\ \# & 0 & \# & \# \end{bmatrix}$$
g^2s^2-6

$$\begin{bmatrix} \# & \# & 0 & 0 \\ \# & 0 & \# & \# \\ \# & 0 & \# & 0 \end{bmatrix}$$
g^2s^2-7

$$\begin{bmatrix} \# & \# & 0 & 0 \\ \# & \# & \# & 0 \\ \# & \# & \# & \# \end{bmatrix}$$
g^2se-1

$$\begin{bmatrix} \# & \# & 0 & 0 \\ \# & \# & \# & 0 \\ \# & \# & 0 & \# \end{bmatrix}$$
g^2se-2

$$\begin{bmatrix} \# & \# & 0 & 0 \\ \# & \# & \# & 0 \\ \# & 0 & \# & \# \end{bmatrix}$$
g^2se-3

$$\begin{bmatrix} \# & \# & 0 & 0 \\ \# & 0 & \# & 0 \\ \# & 0 & \# & \# \end{bmatrix}$$
g^2se-4

$$\begin{bmatrix} \# & \# & 0 & 0 \\ \# & \# & \# & 0 \\ \# & 0 & \# & \# \end{bmatrix}$$
g^2se-5

$$\begin{bmatrix} \# & \# & 0 & 0 \\ \# & \# & \# & 0 \\ 0 & 0 & \# & \# \end{bmatrix}$$
g^2se-6

$$\begin{bmatrix} \# & \# & 0 & 0 \\ \# & 0 & \# & 0 \\ 0 & 0 & \# & \# \end{bmatrix}$$
g^2se-7

$$\begin{bmatrix} \# & \# & 0 & 0 \\ \# & 0 & \# & 0 \\ \# & 0 & 0 & \# \end{bmatrix}$$
g^2se-8

Table 2 Admissible 3-DOF structure matrices

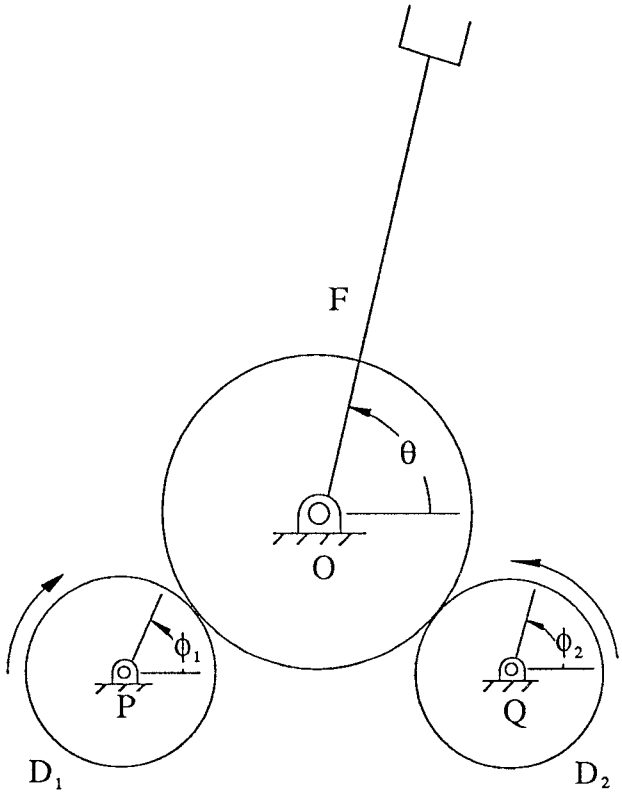

Fig. 1 One-DOF mechanism with redundant unidirectional drives

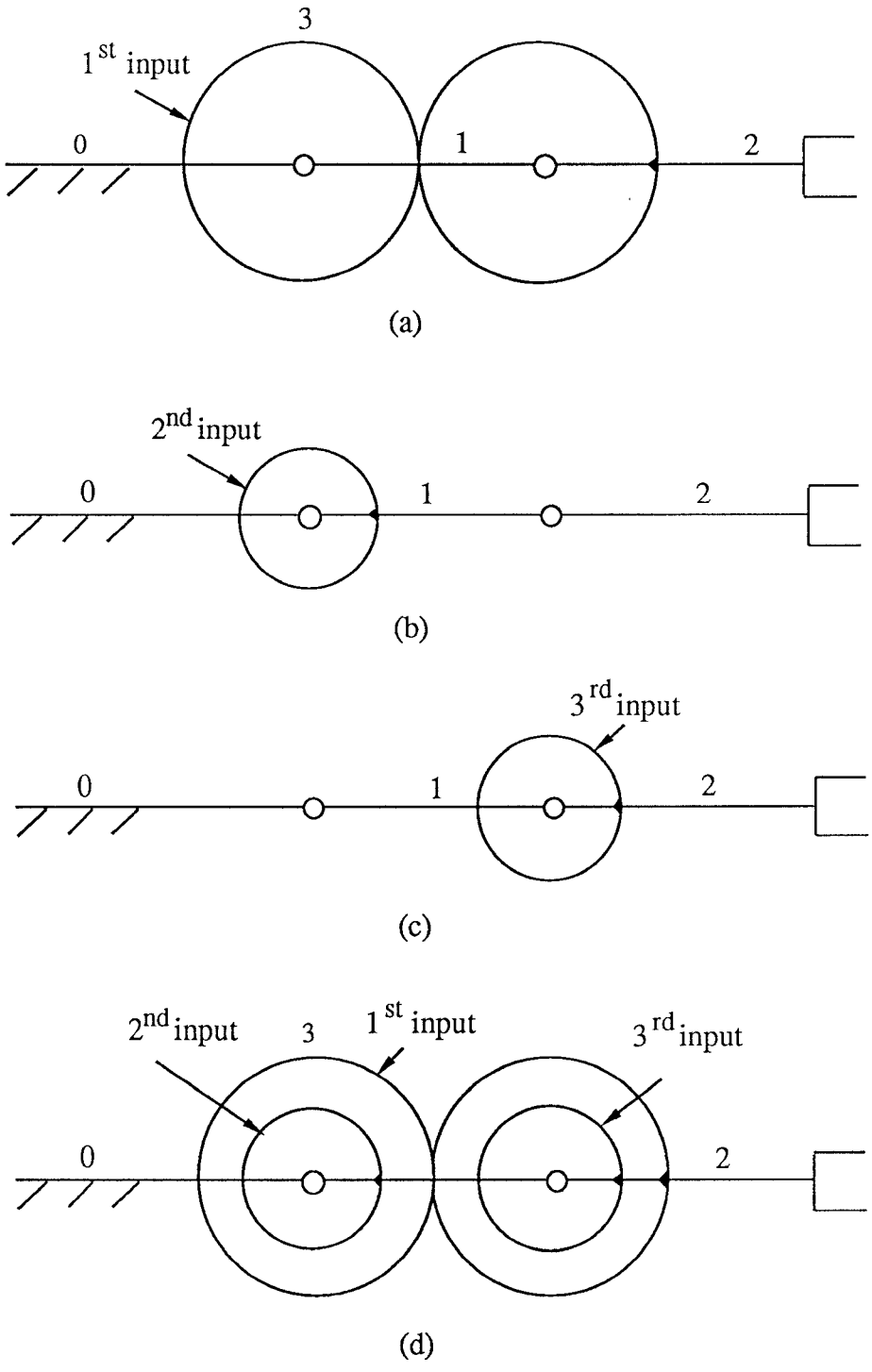

Fig. 2 Construction of the g ^{2}s-2 basic mechanism

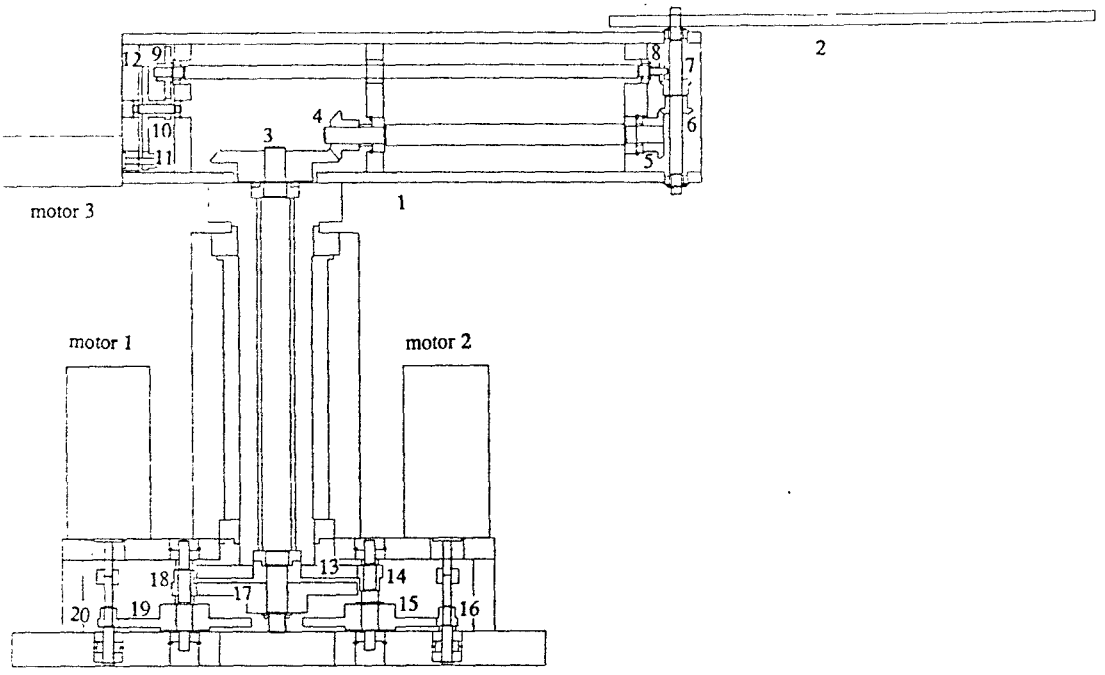

Fig. 3 An experimental 2-DOF manipulator derived from Fig. 2

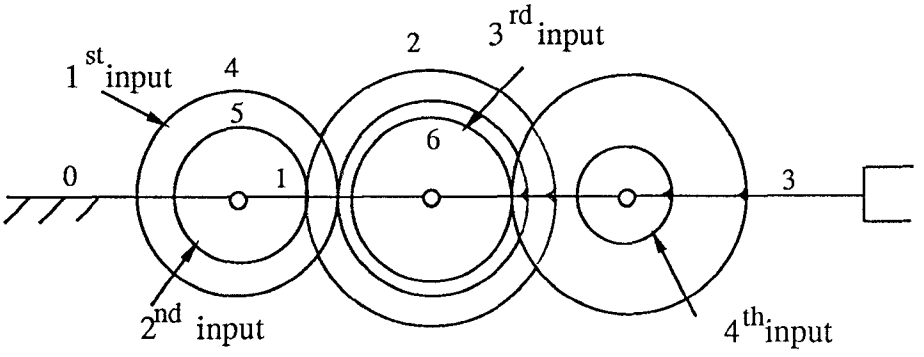

Fig. 4 Construction of the g^2se-6 basic mechanism

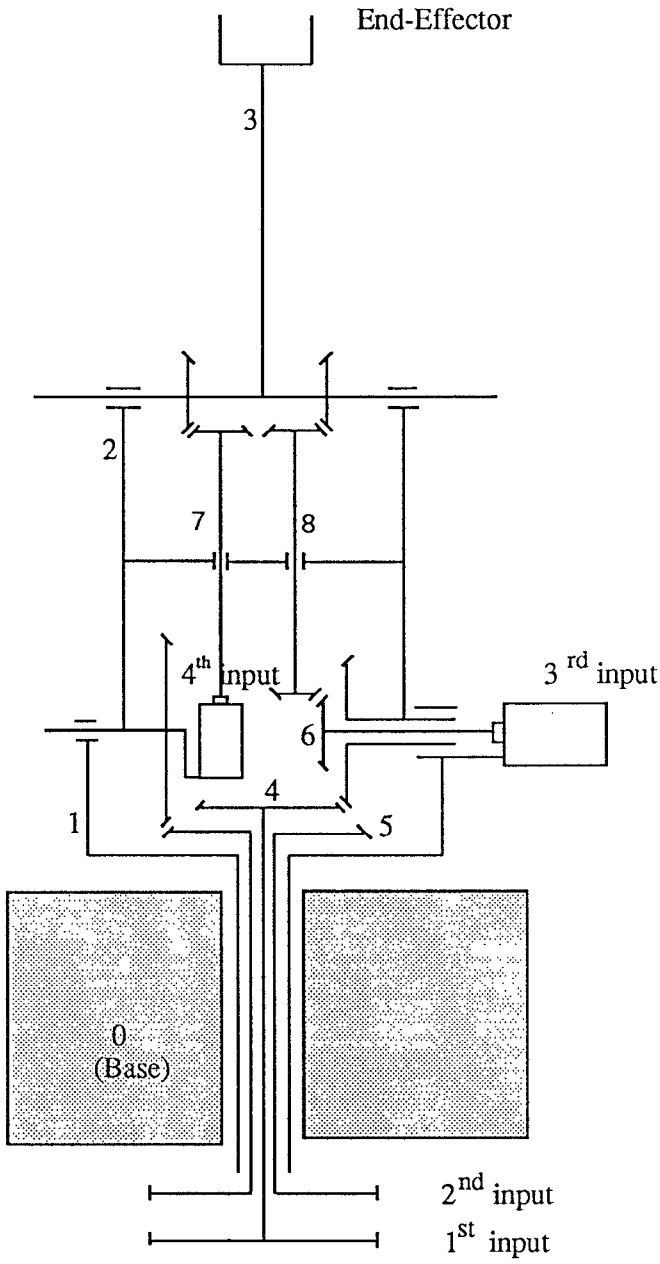

Fig. 5 A spatial 3-DOF arm derived from Fig. 4

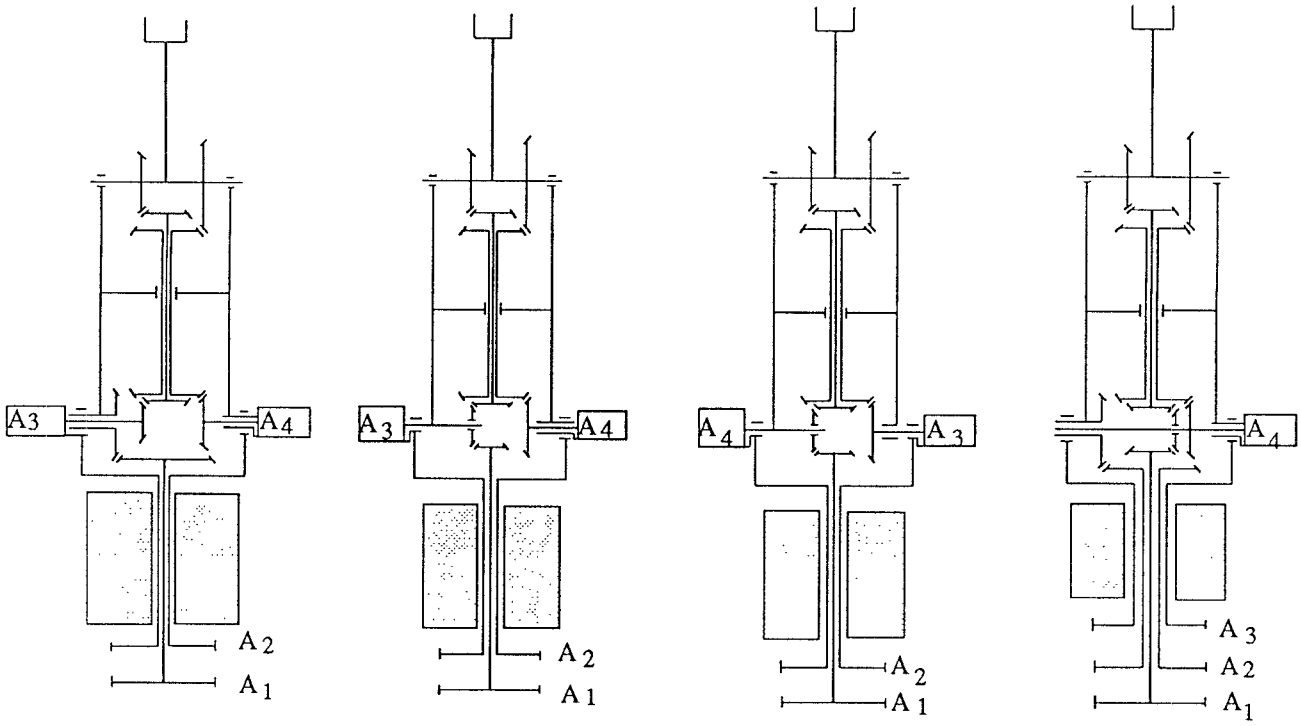

g^2se-7 g^2se-8 g^2s^2-7 g^3e-5

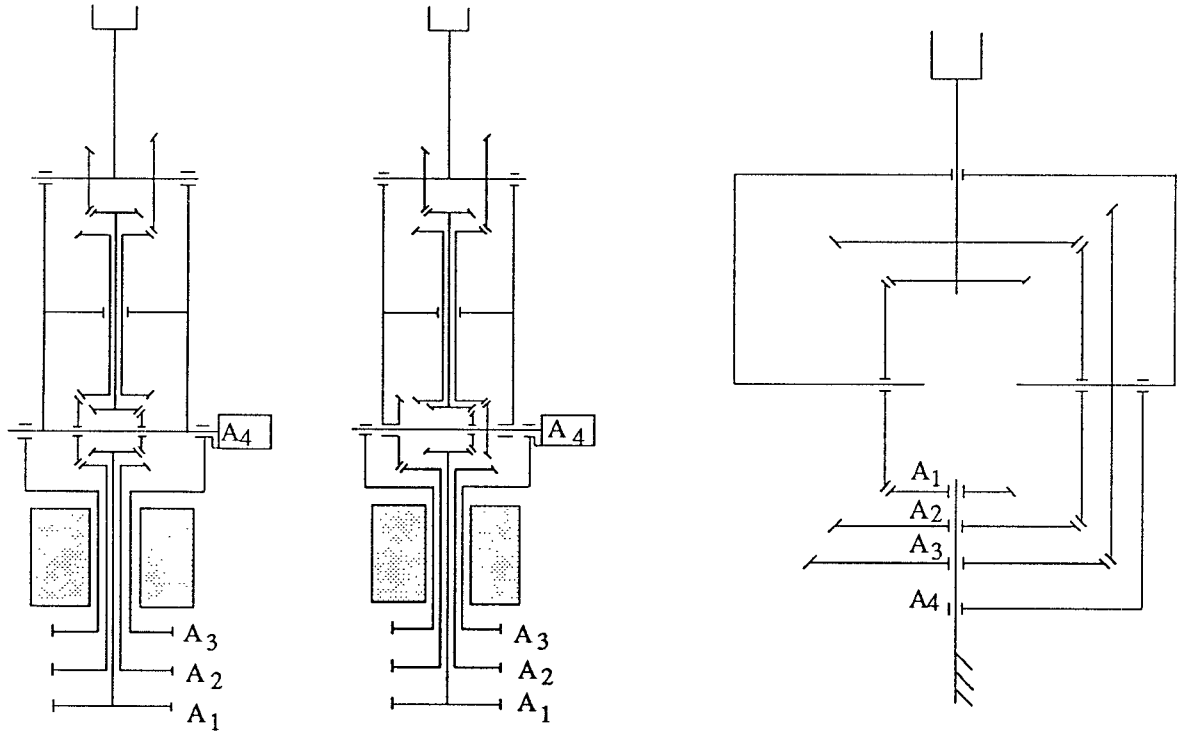

g^3s-7 g^3s-8 g^4-5

Fig. 6 Less coupled 3-DOF robotic mechanisms

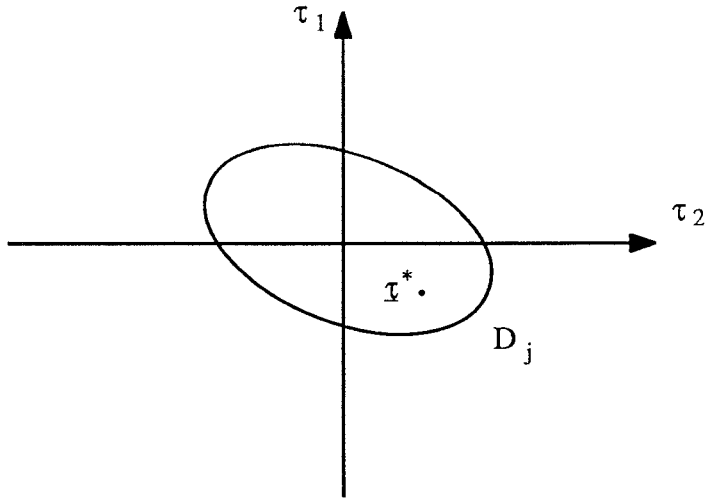

(a)

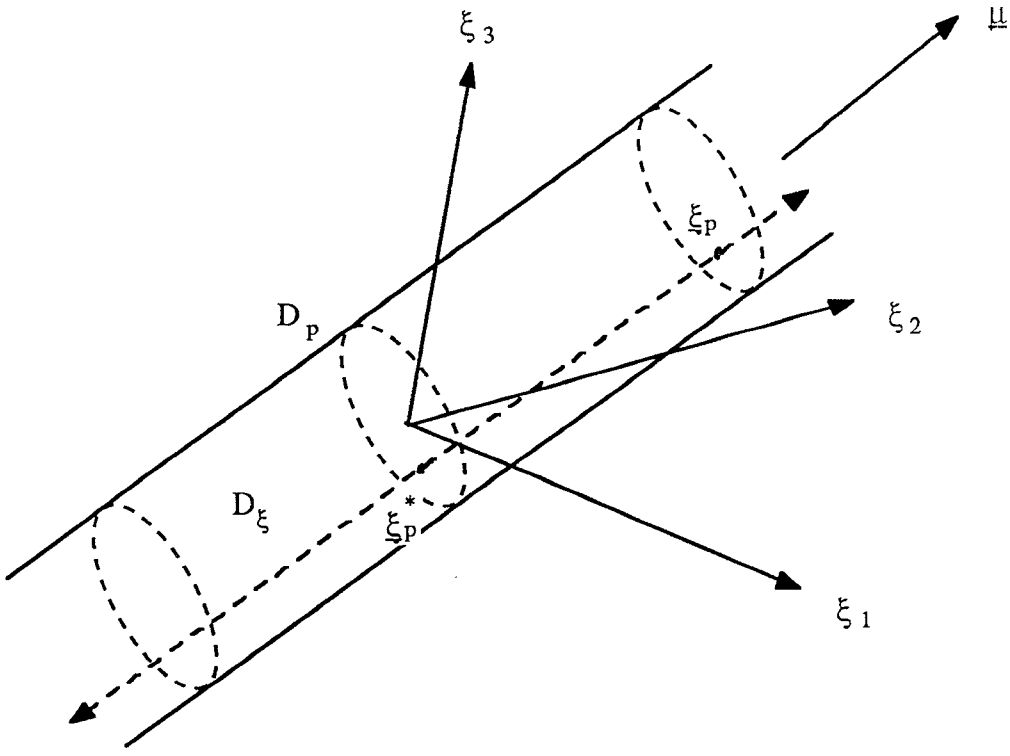

(b)

Fig. 7 The relationship between joint torques and input torques

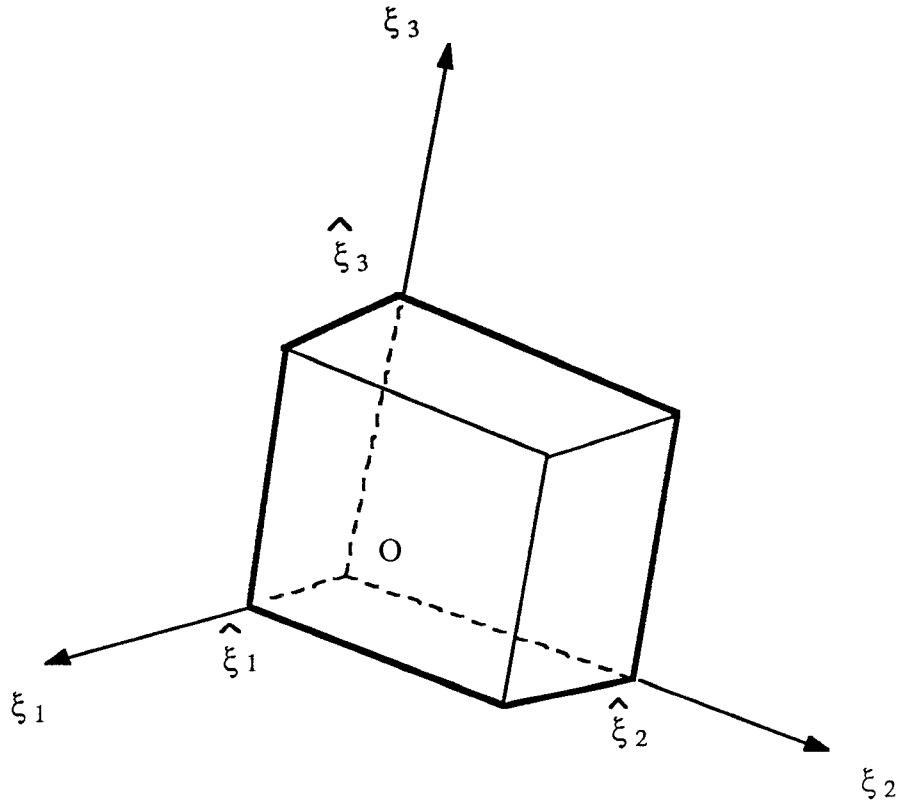

Fig. 8 Available actuator torque domain projected on the particular solution hyperplane

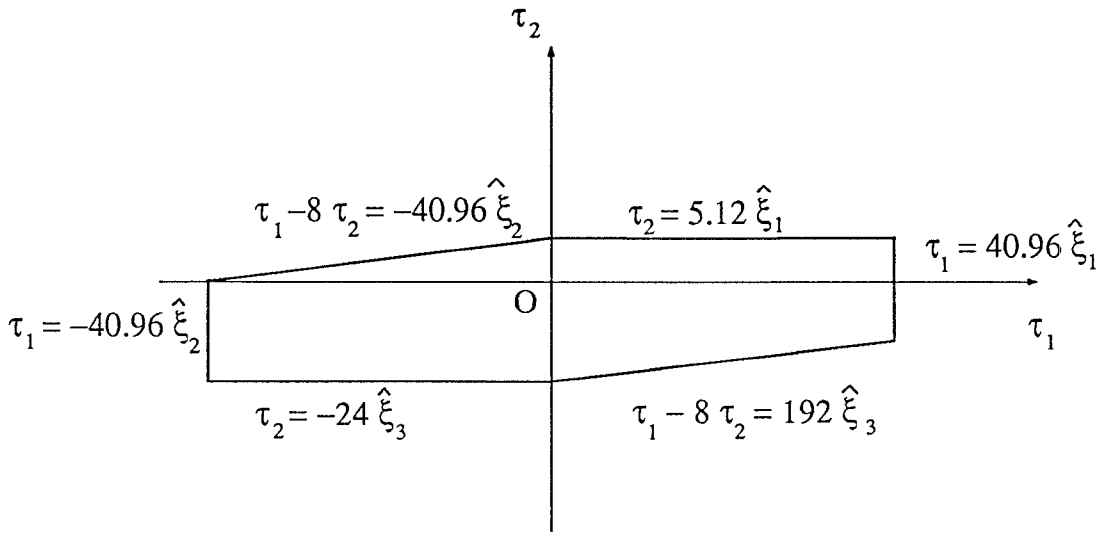

Fig. 9 Domain of available joint torque